

## TREATMENT OF BEAM LOADING EFFECTS IN A STANDING WAVE ACCELERATOR

Masao Kuriki\*, Hisayasu Nagoshi, Tohru Takahashi, AdSM, Hiroshima U., Higashihiroshima, Japan  
Kentaro Negishi, Iwate University, Morioka, Japan  
Yuji Seimiya, Kaoru Yokoya, Masanori Satoh, Accelerator Lab., KEK, Tsukuba, Japan  
Junji Urakawa, RA office, KEK, Tsukuba, Japan  
Tsunehiko Omori, IPNS, KEK, Tsukuba, Japan

### Abstract

ILC (International Linear Collider) is e+ e- linear collider in the next high energy program promoted by ICFA. In ILC, an intense positron pulse in a multi-bunch format is generated by impinging electron beam on a target. The generated positron is captured by a standing wave accelerator in a solenoid focusing. By employing the accelerator with a large aperture, an enough amount of positron can be captured, even with a limited accelerator gradient. However, the heavy beam loading up to 2 A perturbs the field gradient and profile along the longitudinal position. We present the theoretical treatment of the beam loading effect in the standing wave acceleration based on a multi-cell model. Based on the model, we have obtained the expected gradient which is lower than the single cell model. The compensation of the transient beam loading effect is not perfect, but enough for practical use.

### INTRODUCTION

ILC (International Linear Collider) [1] is an e+ e- linear collider with 500 GeV CME in the first phase and 1000 GeV in the second phase. This is only way to realize the e+ e- collision beyond 350 GeV CME beyond the limitation of a storage ring collider and is an official future project promoted by ICFA. It will reveal the structure of Higgs sector which is important to decide the energy scale of the new physics beyond Higgs particle(s). ILC has a high ability to find new physics, such as SUSY particles, dark matter, extra dimensions, etc. ILC realize the high luminosity as high as  $3.0 \times 10^{34} \text{ cm}^{-2} \text{ s}^{-1}$  with a limited average current, 50A. This current is much less than that in a storage ring, but it is larger than that of any conventional linacs. We have to provide 50 A average current by linac. but it is a technical challenge, especially for positron source, because it corresponds to 50 times of that in SLC [2], the first linear collider operated in 1990's.

In the electron driven positron source as shown in Fig. 1, 3 GeV electron beam is used as the driver. The biggest technical challenge is the possible damage on the positron production target. In the ILC beam structure,  $7.8 \times 10^{13}$  positrons are generated in 0.8 ms (macro pulse length). If we assume the same time structure for the positron source, any target can not survive with this heavy thermal heat load and a shock wave induced by the incident beam [3].

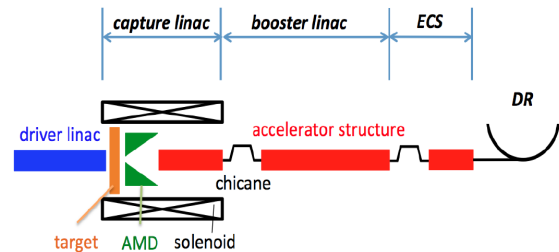


Figure 1: Schematic view of the electron driven ILC positron source. It consists from 3.0 GeV electron driver linac, target, AMD, capture linac, chicane, booster linac, and ECS.

Omori et al. proposed a new e-driven scheme relaxing the target load [4] by extending the effective macro pulse length from 0.8 ms to 64 ms. In this proposal, the positron is generated in 64 ms instead of 0.8 ms. It can be realized by employing a normal conducting linac operated in 300 Hz. One macro pulse contains 66 or 33 bunches in 0.5s and the macro pulse is repeated 20 times in 64 ms period. The heat load on the target can be relaxed much. In the normal conducting accelerator for the positron source, however, a heavy beam loading is expected and this is a new issue. The ILC requirement for the positron intensity is  $2.0 \times 10^{10}$  per bunch at the interaction point, but 50% margin is assumed. The required positron intensity at the positron source is then  $3.0 \times 10^{10}$  per bunch. The positron bunch is accelerated in the booster by 1.3 GHz and 2.6 GHz RF accelerator and the bunch spacing is 6.15ns giving 0.78 A average current in the macro pulse. In addition, additional contributions from electrons and positrons which are not captured is expected at the down stream of the production target. We have to manage this heavy beam loading. In this scheme, positrons are accelerated by normal conducting accelerator and heavy beam loading is expected. Satoh et al. [5] proposed a beam loading compensation for the traveling wave linac by amplitude modulation. Urakawa [6] proposed a fast amplitude modulation method by combining two RF sources with a fast phase switching. Seimiya, Kuriki, et al. [7] showed that an enough positron,  $3.0 \times 10^{10}$  per bunch can be generated by assuming the beam loading compensation.

In this article, we focused on the beam loading treatment of the L-band standing wave structure used in the capture linac (the 1st accelerator section) at the down stream of the target. Usually, a standing wave linac is treated as a single cell cavity and the beam loading for multi-bunch acceleration is perfectly compensated by adjusting the timing

\*mkuriki@hiroshima-u.ac.jp

of the beam acceleration as we will see. The real structure is multi-cell. The cells are coupled to each other. The RF power is fed to the center cell and transferred to the end cell through the structure. On the other hand, the beam loading is induced in each cell. We developed a new model for a standing wave accelerator based on multi-cell. We re-evaluated the accelerator gradient and examined the beam loading compensation based on the model.

In the following sections, we explain the new model starting from the conventional single cell model.

## SINGLE-CELL MODEL OF STANDING WAVE STRUCTURE

Before we discuss the multi-cell mode, the single cell model is p The single cell model of a standing wave tube can be found in many places. The beam loading can be compensated with a appropriate conditions [8]. The voltage of the structure is given as

$$V(t) = \frac{2\sqrt{\beta P_0 r L}}{1 + \beta} \left(1 - e^{-\frac{t}{\tau}}\right) - \frac{r I L}{1 + \beta} \left(1 - e^{-\frac{t-t_b}{\tau}}\right), \quad (1)$$

where  $P_0$  is the input power,  $r$  is a shunt impedance,  $L$  is the length of the structure,  $\beta$  is the coupling coefficient,  $I(A)$  is the beam loading current,  $t_b$  is the timing to start the beam acceleration,  $\tau$  is the filling time of the structure given as

$$\tau = \frac{2Q}{\omega(1 + \beta)} \quad (2)$$

where  $Q$  is Q-value.  $V(t)$  can be constant in time as

$$V = \frac{2\sqrt{\beta P_0 r L}}{1 + \beta} \left(1 - \frac{I}{2} \sqrt{\frac{r L}{\beta P_0}}\right), \quad (3)$$

if the following condition is set as

$$t_b = -\tau \ln \left( \frac{I}{2} \sqrt{\frac{r L}{\beta P_0}} \right). \quad (4)$$

## MULTI-CELL MODEL FOR STANDING WAVE ACCELERATOR

The single cell model is good to understand the standing wave accelerator, but it is not realistic. The real accelerator tube consists from multi-cells and each cells are connected through a finite coupling. As we will see later, the beam loading compensation is still effective, but the accelerator gradient is much less than that expected by the single cell model. Here, we derive the multi-cell model for a standing wave structure [9]. We assume 1.3 GHz 11 cells cavity designed by Wang [10]. The couple is attached at the center cell (cell 0) as shown in Fig. 2. The cavity is symmetric at the couple cell, then we consider only one side, cell 1 to 5. For each cells,  $w_i$ ,  $V_i$ , and  $P_i$  are stored energy, voltage, and dissipated power loss. We assume each cells are idetical, i.e.

$$Q_0 = \frac{\omega W_i}{P_i}, \quad (5)$$

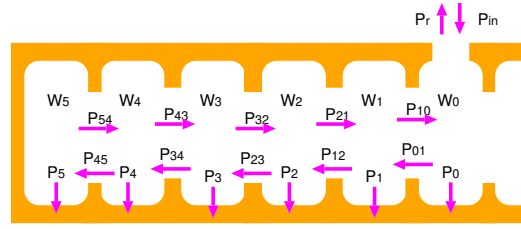


Figure 2: 11 cells standing wave cavity model.

where  $Q_0$  is quality factor and

$$P_i = G V_i^2, \quad (6)$$

where  $G$  is admittance for one cell.

The time differential of  $W_0$  is

$$\frac{dW_0}{dt} = -P_0 - P_{01} - P_{0-1} + P_{10} + P_{-10} + P_{in} - P_r - I V_0, \quad (7)$$

where  $P_{in}$  and  $P_r$  are input power and reflected power from and to the wave guide.  $I V_0$  is the beam loading term. Please note that  $P_{0-1}$  and  $P_{-10}$  are power flow to and from the cell -1. By inserting  $P_{01} = k Q P_0$ ,  $P_{10} = k Q P_1$  to Eq.(7), we get

$$\begin{aligned} \frac{dW_0}{dt} = & -G V_0^2 - 2k Q G V_0^2 + k Q G V_1^2 + k Q G V_{-1}^2 \\ & + G_{wg} V_{in}^2 - G_{wg} (V_{in} - N V_0)^2 - I V_0, \end{aligned} \quad (8)$$

where the power is converted to the voltage.  $V_{in}$  and  $G_{wg}$  are input RF voltage and admittance of wave guide. The wave guide power is defined with the total voltage of the cavity and  $V_0$  is multiplied with  $N$ , number of cells. The admittance of the whole cavity  $G_0$  is  $N$  times smaller than that for one cell  $G$ , then  $G_{wg} = \beta G_0 = \beta G/N$ , we get

$$\begin{aligned} \frac{dW_0}{dt} = & -(1 + N\beta - 2kQ) G V_0^2 + k Q G V_1^2 + k Q G V_{-1}^2 \\ & + 2\beta G V_{in} V_0 - I V_0. \end{aligned} \quad (9)$$

With  $W_0 = \frac{Q}{\omega} G V_0^2$ , the equation becomes

$$\begin{aligned} \frac{dV_0}{dt} = & - \left[ \frac{(1 + N\beta)\omega}{2Q} + k\omega \right] V_0 + \frac{1}{2} k\omega \frac{V_1^2}{V_0} + \frac{1}{2} k\omega \frac{V_{-1}^2}{V_0} \\ & + \frac{\omega\beta}{Q} V_{in} - \frac{\omega R I}{2Q}. \end{aligned} \quad (10)$$

Because the time constant of the cell coupling is much faster than that for the RF fill and RF power decay, we expect  $V_i(t) \sim V_{i\pm 1}(t)$ . Then,  $V_1^2/V_0 \sim V_1$  and  $V_{-1}^2/V_0 \sim V_{-1}$  leads

$$\begin{aligned} \frac{dV_0}{dt} = & - \left[ \frac{(1 + N\beta)\omega}{2Q} + k\omega \right] V_0 + \frac{1}{2} k\omega V_1 + \frac{1}{2} k\omega V_{-1} \\ & + \frac{\omega\beta}{Q} V_{in} - \frac{\omega R I}{2Q}. \end{aligned} \quad (11)$$

In a similar way, we can derive that for cell 1 as

$$\frac{dV_1}{dt} = \frac{1}{2} k\omega V_0 - \left( \frac{\omega}{2Q} + k\omega \right) V_1 + \frac{1}{2} k\omega V_2 - \frac{\omega R I}{2Q}. \quad (12)$$

The equation is almost identical up to cell 4, but that for cell 5 is

$$\frac{dV_5}{dt} = \frac{1}{2}k\omega V_4 - \left(\frac{\omega}{2Q} + \frac{1}{2}k\omega\right)V_5 - \frac{\omega RI}{2Q}. \quad (13)$$

These equations are simultaneous linear differential equations which can be solved with the matrix formalism. The equation in matrix form is

$$\frac{d\mathbf{V}}{dt} = \mathbf{A}\mathbf{V} + \mathbf{C}. \quad (14)$$

The vector  $\mathbf{V}$  is

$$\mathbf{V} = (V_{-5}, \dots, V_{-1}, V_0, V_1, \dots, V_5). \quad (15)$$

The matrix  $\mathbf{A}$  has components as

$$A_{-5,-5} = A_{5,5} = a_5 \quad (16)$$

$$A_{0,0} = a_0 \quad (17)$$

$$A_{ii} = a, \quad (i = 1, 4), \quad (18)$$

$$A_{i,i\pm 1} = \alpha \quad (19)$$

with

$$a_0 = -\frac{(1+N\beta)\omega}{2Q} - k\omega \quad (20)$$

$$a = -\frac{\omega}{2Q} - k\omega \quad (21)$$

$$a_5 = -\frac{\omega}{2Q} - \frac{1}{2}k\omega \quad (22)$$

$$\alpha = \frac{1}{2}k\omega. \quad (23)$$

All components of the vector  $\mathbf{C}$  is

$$C_i = -\frac{\omega RI}{2Q}, \quad (24)$$

except  $C_0$  as

$$C_0 = \frac{\omega\beta}{Q}V_{in} - \frac{\omega RI}{2Q}. \quad (25)$$

$\mathbf{A}$  is a symmetric real matrix which can be diagonalized with a orthogonal matrix  $\mathbf{R}$  as

$$\mathbf{R}^T \mathbf{A} \mathbf{R} = \mathbf{B}, \quad (26)$$

where  $\mathbf{B}$  is a diagonal matrix. With this matrix, Eq. (7) becomes

$$\frac{d\mathbf{R}^T \mathbf{V}}{dt} = \mathbf{R}^T \mathbf{A} \mathbf{R} \mathbf{R}^T \mathbf{V} + \mathbf{R}^T \mathbf{C}. \quad (27)$$

$$\frac{d\mathbf{V}'}{dt} = \mathbf{B}\mathbf{V}' + \mathbf{C}', \quad (28)$$

where  $\mathbf{V}' \equiv \mathbf{R}^T \mathbf{V}$  and  $\mathbf{C}' \equiv \mathbf{R}^T \mathbf{C}$ . Because  $\mathbf{B}$  is a diagonal matrix, the differential equation is simply expressed as

$$\frac{dV'_i}{dt} = \lambda_i V'_i + C'_i, \quad (29)$$

which can be solved as

$$V'_i = \tau_i C'_i + D e^{-\frac{t}{\tau_i}}, \quad (30)$$

where  $\tau_i = -1/\lambda_i$ .  $D$  is an integral constant determined from initial condition. For  $V'(t=0) = 0$ , the solution is

$$V'_i(t) = \tau_i C'_i \left(1 - e^{-\frac{t}{\tau_i}}\right), \quad (31)$$

Once the solution for  $V'$  is obtained, the solution for  $V_i$  is obtained as linear combination of  $V'$  as

$$\mathbf{V} = \mathbf{R}\mathbf{V}'. \quad (32)$$

The solution for the  $i$ -th cell is obtained in the form as

$$V_i(t) = \sum_{j=-5}^5 R_{ij} \tau_j C'_j \left(1 - e^{-\frac{t}{\tau_j}}\right). \quad (33)$$

The total accelerator voltage per the structure is given as the sum of the cell voltage

$$V(t) = \sum_{i=-5}^5 V_i(t). \quad (34)$$

## THE ACCELERATOR PERFORMANCE BASED ON THE MULTI-CELL MODEL

In this section, we extract the accelerator performance based on the multi-cell model. We assume 11 cells L-band (1.3 GHz) standing wave structure designed by J. Wang [10]. The parameter of the structure is summarized in Table 1.

Table 1: Parameters of the L-band Standing Wave Structure Designed by J. Wang [10]

Structure type	Simple $\pi$ mode
Number of Cell	11
Structure Length	1.27 m
Frequency	1.3 GHz
Aperture (2a)	60 mm
Q value	29700
Shunt Impedance	34.3 M/m

Input RF power,  $P_{in}$  is assumed to be 22.5 MW. In this design, 50 MW klystron drives two structures. 10% of the input RF power is lost by wave guide. With zero beam loading,  $I_b = 0A$ , the amplitude of each cell for each mode are calculated. 11 modes are calculated, but only 5 modes have a significant amplitude. The amplitude is shown in Table 2 in MV/cell. The coupling  $\beta$  is assumed to be 6 for the heavy beam loading. Among them, the top mode ( $\tau = 1.22\mu s$  is almost ten times larger than the second mode ( $\tau = 0.068\mu s$ ). Others have a few % or less. The total voltage per structure is 21.6 MV.

The similar table was made for the case with 1.0 A beam loading. We assume no input power at all and the cavity is driven only with the beam. The results are shown in Table 3. The same top 5 modes are shown. The top mode ( $\tau = 1.22\mu s$ ) is more dominant than in 2. This is the main mode which is close to the mode by the single cell model.

Table 2: Amplitude of each cell for top 5 modes with  $I_b = 0$ .  $\tau$  is in  $\mu s$ , and the amplitude is in MV per cell.

$\tau$	0.020	0.006	0.011	0.068	1.22
cell -5	0.063	-0.003	-0.026	-0.232	2.078
cell -4	-0.013	0.010	0.034	-0.149	2.043
cell -3	-0.074	-0.016	0.015	-0.013	1.975
cell -2	-0.045	0.021	-0.039	0.127	1.873
cell -1	0.038	-0.026	-0.002	0.222	1.740
cell 0	0.075	0.030	0.040	0.238	1.578
cell 1	0.038	-0.026	-0.002	0.222	1.740
cell 2	-0.045	0.021	-0.039	0.127	1.873
cell 3	-0.074	-0.016	0.015	-0.013	1.975
cell 4	-0.013	0.010	0.034	-0.149	2.043
cell 5	0.063	-0.003	-0.026	-0.232	2.078

The beam loading power drives each cell, but the RF drives only the center cell, cell 0. The mode by the beam loading is close to that in the single cell. The total voltage is -7.2 MV. The real mode is linear sum of the modes given in

Table 3: Amplitude of each cell for top 6 modes with  $I_b = 1.0$  and no input power.  $\tau$  is in  $\mu s$ , and the amplitude is in MV per cell.

$\tau$	0.020	0.006	0.011	0.068	1.22
cell 0	-0.000	0.000	0.000	0.004	-0.710
cell 1	0.000	-0.000	-0.000	0.002	-0.698
cell 2	-0.000	0.000	-0.000	0.000	-0.674
cell 3	0.000	-0.000	0.000	-0.002	-0.639
cell 4	-0.000	0.000	0.000	-0.004	-0.594
cell 5	-0.000	-0.000	-0.000	-0.004	-0.539
cell 6	-0.000	0.000	0.000	-0.004	-0.594
cell 7	0.00	-0.000	0.000	-0.002	-0.639
cell 8	0.000	0.000	-0.000	0.000	-0.674
cell 9	0.000	-0.000	-0.000	0.002	-0.698
cell 10	-0.000	0.000	0.000	0.004	-0.710

Table 2 and 3 by accounting the input RF power and the beam loading current. Figure 3 shows the voltage evolution based on the multi-cell model by assuming 22.5 MW input with parameters in Ref. [10]. The dotted line is voltage by RF, the dashed line is 2.0 A beam-loading, and the solid line is the total voltage. The timing to start the acceleration is manually adjusted to give the voltage as flat as possible. As you can see, the beam loading compensation is quite efficient. The reason can be understood because only few modes contribute to the acceleration. The fluctuation is less than 0.1% [9]. Figure 4 shows the voltage per tube as a function of coupling  $\beta$  for various loading currents. The same conditions are assumed. Table 4 shows a comparison of voltage by the single cell model and multi-cell model.

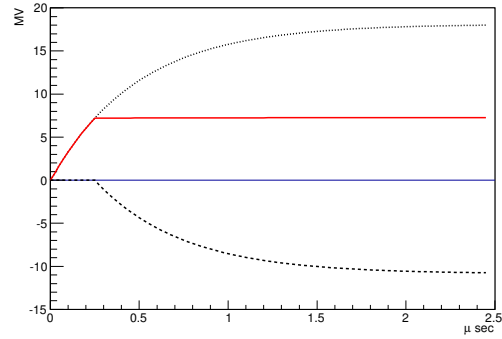


Figure 3: The voltage evolution obtained with the multi-cell model with 2.0 A beam loading. The solid, dotted, and dashed lines show total voltage, RF and beam-loading contributions, respectively.

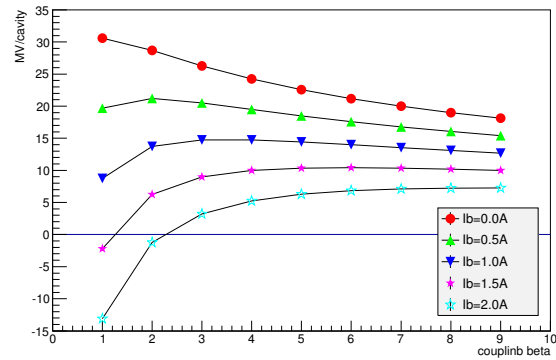


Figure 4: The voltage as a function of coupling  $\beta$  for various loading currents.

There is a large discrepancy in the heavy load, because the beam loading compensation with the external load is less for the multi-cell model.

Table 4: Accelerating Voltage by Two Models

Beam loading (A)	Single cell (MV)	Multi-cell (MV)
0 A	18.7	21.6
1 A	14.4	14.4
2.0 A	10.1	7.2

## SUMMARY

We have developed a multi-cell model for standing wave structures. The structure is modeled as multi-cells coupled to the next cell each other. The voltage becomes less than that by the single cell mode with a heavy beam loading, because the external load is less effective to compensate the beam loading in the multi-cell model. The beam loading compensation is still working well with a heavy beam loading, because a few modes are dominant.

## **ACKNOWLEDGEMENT**

This study is partly supported by the Quantum beam Project by the Ministry of Education, Culture, Sports, Science and Technology, entitled High Brightness Photon Beam by Laser-Compton Scattering and Cooperative supporting program for Researches and Educations in University by KEK (High Energy Accelerator Research Organization).

## **REFERENCES**

- [1] ILC Technical Design Report (2013).
- [2] SLC Design Handbook, SLAC Report (1984).
- [3] M. Kuriki *et al.*, PRSTAB **9**, 071002(2006).
- [4] T. Omori *et al.*, NIMA(672)(2012)52.
- [5] M. Satoh *et al.*, NIMA538(2005)116-126.
- [6] J. Urakawa, Posipol 2014, Ichinoseki, Japan(2014).
- [7] Y. Seimiya *et al.*, PTEP. (2015) 103G01.
- [8] Handbook of acc. phys. and eng., World Scientific(1998).
- [9] M. Kuriki *et al.*, *Proc. of PASJ*, WEOM06(2016).
- [10] J.W. Wang *et al.*, SLAC-PUB-12412(2007).